Two-frequency excitation, anisotropy of the intensity, and effects of asymmetry of the tensor of hyper-Raman light scattering in crystalline quartz

V. N. Denisov, B. N. Mavrin, V. B. Podobedov, and Kh. E. Sterin

Institute of Spectroscopy, Academy of Sciences of the USSR, Troitsk, Moscow Province
(Submitted 24 June 1985; resubmitted 4 September 1985)
Zh. Eksp. Teor. Fiz. **90**, 581–589 (February 1986)

The hyper-Raman scattering (HRS) of light was observed for the first time under two-frequency excitation conditions, i.e., using simultaneously two laser beams of different wavelengths (1064 and 532 nm). The polarized HRS spectra were obtained for α-quartz, and the anisotropy of the HRS intensity in the case of mixed vibrations was observed and explained. A study was made of the effects of asymmetry of the HRS tensor: the HRS spectra were observed for A_1 (201 and 464 cm^{-1}) vibrations in geometries allowed only for the asymmetric part of the tensor and the HRS intensity was affected by transportation of the tensor indices. Although the frequencies of the exciting and scattered light were located far from the electronic absorption bands of quartz, the contribution of the asymmetric part of the tensor to the HRS intensity was still important.

I. INTRODUCTION

The hyper-Raman scattering (HRS) of light is now widely used in studies of vibrational states of matter, alongside the classical methods of Raman scattering (RS) and infrared (IR) absorption spectroscopy. Since the selection rules are different for these processes, the methods in question can successfully complement one another. In contrast to RS and IR absorption, HRS is a nonlinear process and is due to the quadratic term of an expansion of the induced polarization in powers of the field intensity of the exciting wave. A quantum-mechanical study of the components of the HRS tensor $\beta_{mnl}(\omega_s, \omega_{i1}, \omega_{i2})$, where the indices s and i represent the scattered and incident (exciting) light, respectively, are reported in Refs. 1–4.

A correct interpretation of the RS and HRS spectra requires the knowledge of the symmetry properties of the scattering tensor. It has been found in practice that the Placzek conditions[5] ($\omega_s \gg \omega_k$ and $\omega_\alpha - \omega_s \gg \omega_k$, where ω_α and ω_k are, respectively, the frequencies of electronic and vibrational transitions) ensure that the RS tensor is symmetric and the RS spectra can then be analyzed ignoring the antisymmetric part of the scattering tensor. The problem of the symmetry of the HRS tensor has not yet been solved. On the one hand, the HRS spectra are being interpreted assuming complete symmetry of the HRS tensor, which simplifies the analysis. On the other hand, according to Refs. 1–4, the tensor β_{mnl} is asymmetric and the conditions for the symmetry of the HRS tensor are much more stringent than the restrictions which have to be imposed to make the RS tensor symmetric. In terms of the Placzek approximation, the HRS tensor is generally ($\omega_{i1} \neq \omega_{i2}$) symmetric only in respect of the last two indices, but for $\omega_{i1} = \omega_{i2}$ the tensor does not acquire new symmetry properties. It becomes completely symmetric only for $\omega_s, \omega_i \ll \omega_\alpha$. Since in real experiments we have $\omega_s, \omega_i \gtrsim 0.3\omega_\alpha$, the asymmetric part $\bar{\beta}_{mnl}$ of the HRS tensor may be large. We are not aware of experimental investigations of the contribution of $\bar{\beta}_{mnl}$ to the HRS spectra. An allowance for $\bar{\beta}_{mnl}$ not only makes tensor components differing with transposed the indices unequal, but may give rise to new components which vanish in the case of a totally symmetric tensor β^s_{mnl}. Moreover, some vibrational modes may be active in HRS only because of this asymmetric part, so that when allowance is made for $\bar{\beta}_{mnl}$ the spectroscopic applications of the HRS method become much more extensive.

We shall consider the contribution of $\bar{\beta}_{mnl}$ to the HRS spectra of crystalline quartz (α-SiO_2). The HRS spectra of α-SiO_2 had not been determined before, basically because of their extremely low intensity, although the vibrational spectra had been investigated thoroughly by other methods, such as RS,[6] IR absorption,[7] and inelastic neutron scattering.[8]

We shall now consider the selection rules for the symmetric and asymmetric parts of the HRS tensor of α-quartz (Sec. 2) and demonstrate the need to develop a method for two-frequency excitation of HRS, first implemented by us (Sec. 3). In Sec. 4 we shall describe the polarized HRS spectra of α-quartz and the anisotropy of the HRS intensity on rotation of a crystal by 180°. We shall discuss the effects of asymmetry of the HRS tensor of α-quartz in Sec. 5.

2. SELECTION RULES

The structure of an α-SiO_2 crystal is described by the noncentrosymmetric space group $D_3(z = 3)$. The vibrational representation of such a crystal is classified in accordance with irreducible representations $4A_1 + 4A_2 + 8E$, out of which the vibrations of the A_1 and E classes are active in RS, A_2 and E in infrared absorption, whereas A_1, A_2, and E in HRS.

A completely symmetric HRS tensor β^s_{mnl} has a total of ten components[4,9]: $\beta^s_{xxx}, \beta^s_{xyy}, \beta^s_{xzz}, \beta^s_{yxx}, \beta^s_{yyy}, \beta^s_{yzz}, \beta^s_{xxx}, \beta^s_{zyy}, \beta^s_{zzz}, \beta^s_{xyz}$. In the matrix representation the completely symmetric HRS tensors β^s_{mnl} of the vibrations of α-quartz are described by

$$A_1 = \begin{pmatrix} a & -a & \cdot \\ \cdot & \cdot & \cdot \\ \cdot & \cdot & \cdot \end{pmatrix}, \quad A_2(z) = \begin{pmatrix} \cdot & \cdot & \cdot \\ -b & b & \cdot \\ d & d & c \end{pmatrix},$$

 0038-5646/86/020338-06$04.00

$$\bar{E}(x)=\begin{pmatrix} e & {}^1/_3 e & f \\ \cdot & \cdot & \cdot \\ \cdot & \cdot & \cdot \end{pmatrix}, \quad E(y)=\begin{pmatrix} \cdot & \cdot & \cdot \\ {}^1/_3 g & g & h \\ m & -m & \cdot \end{pmatrix}.$$

In the case of the $E(x)$ vibrations the HRS tensor has also a nonzero component β^s_{xyz}.

If, for the sake of simplicity, we shall confine ourselves to a matrix representation which gives the nonzero components, but generally ignores a likely inequality of the tensor components with transposed indices, we find that the asymmetric parts of the HRS tensor $\bar{\beta}_{mnl}$ (Ref. 4) for these vibrations can be represented by

$$\bar{A}_2(z)=\begin{pmatrix} \cdot & \cdot & \cdot \\ \cdot & \cdot & \cdot \\ n & n & \cdot \end{pmatrix}, \quad \bar{E}(x)=\begin{pmatrix} \cdot & p & r \\ \cdot & \cdot & \cdot \\ \cdot & \cdot & \cdot \end{pmatrix},$$

$$\bar{E}(y)=\begin{pmatrix} \cdot & \cdot & \cdot \\ q & \cdot & s \\ t & -t & \cdot \end{pmatrix}.$$

In the case of the $E(x)$ vibrations the asymmetric part of the tensor $\bar{E}(x)$ has also nonzero components $\bar{\beta}_{xyz}=\bar{\beta}_{yzx}$. In the case of the A_1 vibrations the tensor $\bar{\beta}_{nml}$ has only nonzero components $\bar{\beta}_{xyz}=-\bar{\beta}_{yzx}$.

It follows from these selection rules that all the vibrational modes of α-quartz are HRS-active already in the approximation of a totally symmetric tensor. Therefore, the effects of asymmetry of the HRS tensor of α-quartz can be detected only by investigating the intensities of the spectra in the case of transposition of the indices of the tensor, and also through the appearance of bands in the HRS spectra in the case of those scattering geometries when the bands are forbidden in the approximation of a totally symmetric tensor.

A comparison of the tensors β^s_{nml} and $\bar{\beta}_{nml}$ of α-quartz shows that $\bar{\beta}_{nml}$ has nonzero components which vanish in β^s_{nml} only for the A_1 vibrations. It is worth noting that these components ($\bar{\beta}_{xyz}=-\bar{\beta}_{yzx}$) contribute to HRS only in the case of mutually orthogonal polarizations of a pair of exciting photons participating in the HRS process. Detection of this contribution is possible only in the case of two-frequency excitation of the HRS spectra when pairs of exciting photons have different frequencies ($\omega_{i1}\neq\omega_{i2}$). One-frequency excitation of HRS by two beams with orthogonal polarizations gives rise not only to HRS spectra of the kind excited by two beams with orthogonal polarizations, but also to spectra excited separately by each of the beams. Therefore the observed spectra become so complicated by the superposition of bands due to different scattering geometries, that the search for the asymmetric part of the tensor becomes very difficult if not impossible.

3. EXPERIMENTAL METHOD

Since in the case of two-frequency excitation the HRS intensity is proportional to the product of the intensities of beams of frequencies ω_{i1} and ω_{i2}, it was necessary to ensure the maximum possible powers at both frequencies. Our ω_{i1} and ω_{i2} beams were produced by a single-mode pulsed YAG laser emitting at the fundamental ($\lambda_{i1}=1064$ nm) and second-harmonic ($\lambda_{i2}=532$ nm) frequencies. The YAG laser

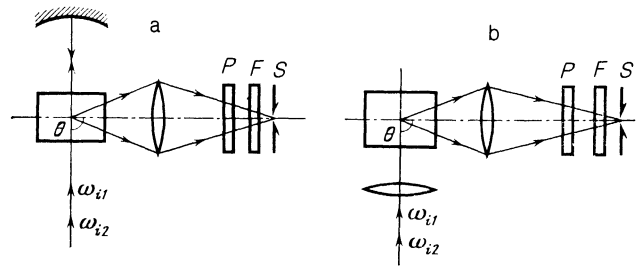

FIG. 1. Schemes used in two-frequency excitation of HRS. Here, P is a polarizer, F is an UFS-1 filter, and S is a spectrograph slit.

was constructed from two active elements, each 100 mm long and 5 mm in diameter, placed in series in a shared resonator. Frequency doubling took place in an $LiIO_3$ crystal which was 20-mm long and placed outside the resonator. When the pulse repetition frequency was ~ 4 kHz, the peak powers were $P_{i1}=30$ and $P_{i2}=10$ kW, whereas the average powers were 12 and 3 W, respectively.

At the exit from the laser the ω_{i1} and ω_{i2} radiations had mutually orthogonal polarizations. The various scattering geometries were realized by rotating the planes of polarization of the ω_{i1} and ω_{i2} beams using thin sapphire plates.

The intensity in the HRS spectra obtained by two-frequency excitation was critically sensitive to the precision of spatial coincidence of the ω_{i1} and ω_{i2} exciting beams, i.e., to the coincidence of the "constrictions" of the two beams inside a sample. The optimal conditions for the excitation of HRS were found by testing two schemes. In the first (Fig. 1a) the two unfocused beams passed through a sample and were returned to the sample by a concave mirror ($F=40$ mm). In the second scheme (Fig. 1b) the beams were focused inside a sample by a lens ($F=35$ mm) which, because of chromatic aberration, introduced an additional mismatch in respect of the constriction positions. Against expectations, the first scheme showed no major advantages. Therefore, the second scheme was preferred because of the simpler alignment procedure.

The scattered light was analyzed with a spectrograph ($F/7$) characterized by a resolution (with the recording system included) reaching 7 cm^{-1}. The HRS spectra were recorded by a multichannel photoelectric system with the main elements described in Ref. 10. The peak intensities of the strongest lines did not exceed 2–3 photoelectrons per second per a resolved interval. Therefore, reliable recording of weak lines required accumulation of the signal in the memory of an external digital store for a period of 40 min. A spectral interval ~ 400 cm^{-1} wide was recorded simultaneously.

4. HYPER-RAMAN SPECTRA OF α-QUARTZ

4.1. Polarized HRS spectra

In the case of two-frequency excitation the HRS spectra are located close to the sum of the frequencies of the exciting radiations ω_{i1} and ω_{i2}, where in the case of the noncentrosymmetric crystal of α-SiO_2 we can expect also the scattering of light by optical vibrations due to cascade (multistage)

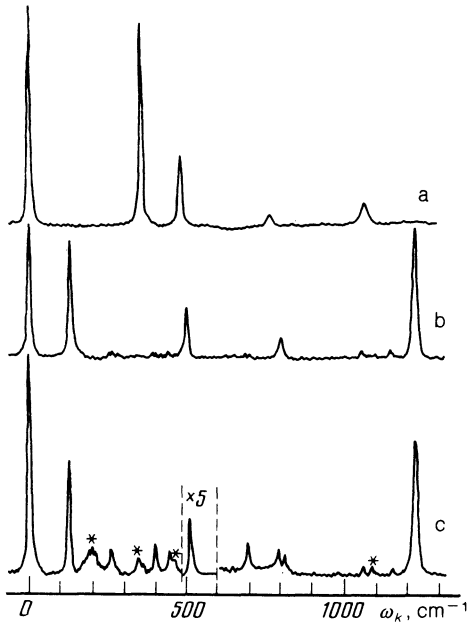

FIG. 2. Polarized HRS spectra of α-quartz obtained for different scattering geometries: a) $x(zzz)y$ (A_2 vibration); b) $x(zyy)y$, $[E(TO)+E(LO)]$; c) $x(xyy)y[A_1+E(TO)+E(LO)]$. The asterisks are used for the A_1 vibrations. The following notation is used for the scattering geometries: the symbols inside the parentheses are the directions of propagation of the exciting light (to the left of the parentheses) and of the scattered light (to the right of the parentheses); inside the parentheses the first symbol represents the polarization of the scattered light and the next two symbols represent the polarizations of the exciting light.

processes consisting of two consecutive stages, one of which is RS or HRS and the other is sum-frequency generation. In our experiments, HRS was not excited in α-quartz. It was shown by us in detail on an earlier occasion (first part of Ref. 4) that in the case of the cascade processes involving RS the intensities were much less than the HRS intensity if the exciting radiation was far from the phase matching (this was true of our experiments) and the scattered light was observed for the scattering angle of 90°. The negligibly small contribution of the cascade processes to the HRS spectra of α-SiO_2 was confirmed also by other features of these spectra: a) the polarizations of bands due to various vibrational modes (A_1, A_2, and E) obeyed the selection rules for HRS (Sec. 2 and Fig. 2); b) the ratio of the band intensities was different from that in RS spectra [for example, the strongest RS band at 466 cm^{-1} (class A_1) was one of the weakest bands in HRS (Fig. 2c)]; c) the most important feature was that the recorded spectra had strong bands due to the A_2 vibrations (Fig. 2a) forbidden in the case of RS (including the cascade processes involving RS), but active in HRS (Sec. 2).

The A_2 vibration forbidden in RS was of the greatest interest in the study of HRS of α-quartz. When the scattering angle was 90°, it was possible to observe only the TO components of the A_2 vibrations (Fig. 2a). Out of four bands of the TO modes, the strongest was the band at 362 cm^{-1}. It was observed reliably also for other scattering geometries when the HRS intensity was governed by the tensor components β_{yxx} and β_{zxx}. It should be pointed out that the HRS intensities of the A_2 vibrations were correlated with the oscillator strengths of these modes. For example, the 362 cm^{-1} vibration corresponded to the highest oscillator strength, whereas the 772 cm^{-1} vibration corresponded to the lowest strength.[7]

In the HRS spectra of vibrations of the E class (Fig. 2b) the strongest was the band at 1230 cm^{-1}, which was one of the weakest in RS. It corresponded to the highest-frequency LO vibration. In this connection it should be noted that the high-frequency LO vibration was usually very strong in HRS, as found also in the spectra of other crystals ($SrTiO_3$, TiO_2, $CaCO_3$, $LiNbO_3$, $LiTaO_3$, etc.).

The HRS spectra of totally symmetric A_1 vibrations could be recorded only simultaneously with the E vibrations and, in contrast to the RS spectra,[6] they were very weak (Fig. 2c). The soft mode at 201 cm^{-1} had the highest integrated intensity among these vibrations.

The data on the HRS spectra of α-quartz are presented in Table I.

4.2. Anisotropy of the intensities in hyper-Raman spectra

A study of mixed vibrations of α-quartz revealed an anisotropy of the intensity of HRS when a crystal was rotated by 180° about crystallographic axes. For example, in the scattering geometry $y(yxx+xxx)z$ in which the polarization of the scattered light was not analyzed, the intensities of mixed $A_2(TO)+E(TO)$ vibrations (467 cm^{-1} band) and of $A_2(LO)+E(LO)$ vibrations (544 cm^{-1}) changed significantly on rotation of a crystal by 180° about the y axis, re-

TABLE I. Vibration frequencies of α-quartz (cm^{-1}) detected in HRS spectra and their interpretation

Frequency	Vibrational mode	Frequency	Vibrational mode
128	$E(TO+LO)$	201	A_1
265	$E(TO+LO)$	356	
402	$E(LO)$	464	
450	$E(TO)$	1085	
512	$E(LO)$		
695	$E(TO+LO)$	362	$A_2(TO)$
795	$E(TO)$	490	
810	$E(LO)$	772	
1065	$E(TO)$	1072	
1155	$E(TO+LO)$		
1230	$E(LO)$		

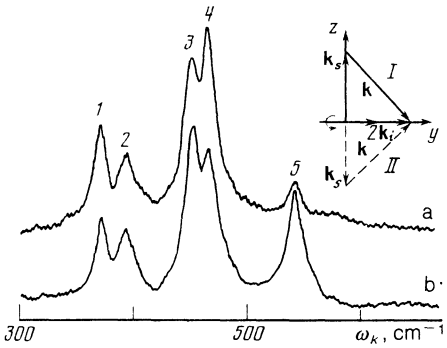

FIG. 3. Hyper-Raman spectra of α-quartz obtained for mixed vibrations in the scattering geometries differing in respect of rotation of a crystal by 180° around the y axis: a) $y(yxx+xxx)z$; b) $y(yxx+xxx)\bar{z}$; 1) $A_2(TO)+A_2(LO)$; 2), 3) $E(TO)$; 4) $A_2(TO)+E(TO)$; 5) $A_2(LO)+E(LO)$.

sulting in establishment of the $y(yxx+xxx)\bar{z}$ geometry (Fig. 3). On the other hand, the intensities of the transverse vibration $E(TO)$ and of the mixed vibration $A_2(TO)+A_2(LO)$ were not affected. In both geometries the intensities of HRS were governed by the same tensor components. However, these geometries differed in respect of the directions of the wave vectors **k** of perturbed vibrations (inset in Fig. 3).

We shall now consider the cause of the observed anisotropy of the HRS intensities. If a vibration is the sum of other vibrations [for example, the doubly degenerate vibration $E(x)+E(y)$ or the mixed vibration $A(z)+E(x)$, etc.], then its intensity in the spectrum is governed by an algebraic sum of the weighted tensor components of each of the vibrations. For example, in the case of the quasitransverse modes $A(z)+E(y)$ this sum is of the form

$$\beta=\beta_A e^z+\beta_E e^y,$$

where β_A and β_E are the tensor components of the vibrations A and E; e^z and e^y are the projections of the unit polarization vector **e** of a quasitransverse vibration along the directions of polarization of the vibrations A and E, respectively. In the case of a quasitransverse vibration, we have **e**⊥**k**. Rotation of a crystal by 180° about the y axis does not alter the projection e^z, but it reverses the sign of e^y. Consequently, whereas before rotation we have $\beta\propto(\beta_A+\beta_E)$, after rotation we find that $\beta\propto(\beta_A-\beta_E)$ for $\theta=90°$. Therefore, if the directions of polarizations of the mixed vibrations are different, the sum of the tensor components may be affected by rotation of a crystal by 180°.

A similar effect had been observed earlier in the Raman scattering spectra.[11] The intensity anisotropy in the HRS spectra can be expected more frequently than in the case of the RS spectra and it is possible in the case of transverse and longitudinal doubly degenerate vibrations, as well as in the case of mixed quasitransverse and quasilongitudinal vibrations. The postulated cases of the anisotropy of the HRS intensity in the $\theta=90°$ case were analyzed by us and are listed for uniaxial crystals in Table II. It should be pointed out that this effect does not occur in cubic crystals or in the case of mixed longitudinal-transverse vibrations in uniaxial crystals.

5. ASYMMETRY OF THE HYPER-RAMAN SCATTERING TENSOR

5.1. Appearance of new nonzero components

It is shown in Sec. 2 that new nonzero components due to the asymmetric part of the HRS tensor can appear only for A_1 vibrations of α-quartz ($\beta_{xyz}=-\bar{\beta}_{yzx}$ components). The HRS due to this tensor component can be observed only by eliminating other possible scattering channels resulting from some depolarization of light and insufficiently accurate orientation of a crystal.

We investigated crystals of high optical quality oriented along the crystallographic axes (misorientation of the axes $\lesssim 0.5°$). Therefore, the directions of the exciting beams and of the scattered light could be selected along a given axis to within 0.5–1°. The orientations of the planes of polarization of the ω_{i1} and ω_{i2} beams relative to the crystallographic axes could be set to within $\lesssim 3°$. In practice the greatest error in the analysis of the polarized scattered-light spectra was due to the finite angle of gathering of the scattered light because of which the deviation of the rays in the scattered light from the direction of observation along the selected axis could

TABLE II. Point groups of uniaxial crystals with HRS spectra expected to exhibit intensity anisotropy, and observation conditions

Point groups	Components of HRS tensors*	Orientation of vibrational wave vector	Rotation axis	Vibrational modes**
C_3, C_{3i}	xy^2, xz^2, yx^2, yz^2, zx^2, zy^2	$x0y$	x, y	TO_x+TO_y, LO_x+LO_y
	x^3, y^3, xz^2, yx^2, yz^2, zx^2, zy^2	$x0z$	x, z	TO_z+TO_x, LO_z+LO_x
	x^3, y^3, xy^2, xz^2, yz^2, zx^2, zy^2	$y0z$	y, z	TO_z+TO_y, LO_z+LO_y
D_3, D_{3d}, C_{3v}	y^3, zx^2, zy^2	$y0z$	y, z	TO_z+TO_y, LO_z+LO_y
C_4, C_{4h}, S_4	xy^2, yx^2, xz^2, yz^2	$x0y$	x, y	TO_x+TO_y, LO_x+LO_y
C_6, C_{3h}, C_{6i}	xy^2, xz^2, yx^2, yz^2	$x0y$	x, y	TO_x+TO_y, LO_x+LO_y

*Simplified notation is used for the tensor components: xy^2 denotes β_{xyy}, etc.

**The indices of the TO and LO vibrations indicate the polarization of the excited phonons.

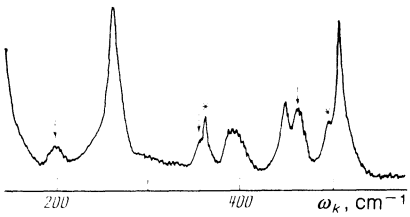

FIG. 4. Hyper-Raman spectra of α-quartz in the $x(xyz)y$ geometry: the arrows identify the A_1 vibrations and the asterisks are used for the A_2 vibrations. The other bands represent the E vibrations.

reach $\pm$ 6–8°. The fraction of light ΔI_0 originating from the other polarization for the line intensity I_0 was estimated as follows:

$$\Delta I_0/I_0 \lesssim \sin^2\varphi < {}^1/_{25},$$

where φ is the maximum deviation of the direction from the selected one ($\varphi \sim 10$–$12°$).

Since α-quartz is optically active, the plane of polarization of the transmitted light should be rotated. However, this effect was significant only when light traveled along the optic axis.[12] Therefore, in our study of the asymmetry the exciting and scattered beams were directed at right-angles to the optic axis when the influence of the optical activity and anisotropy of the crystal on the depolarization of light could be ignored. We therefore selected the $x(xyz)y$ geometry in which in addition to the $\bar{A}_1$ vibrations we expected also activity of the $E(TO)$ and $E(LO)$ vibrations.

Figure 4 shows the HRS spectrum in the frequency range where three bands of the $\bar{A}_1$ vibrations at 201, 356, and 464 cm^{-1} were expected. Only two of them—201 and 464 cm^{-1}—were detected reliably. The 356 cm^{-1} band was close to 362 cm^{-1}, representing the A_2 vibration. It was pointed out in Sec. 4.1 that the intensity of the 362 cm^{-1} band was quite high and, since light could penetrate from other scattering geometries, its appearance as well as that of the 490 cm^{-1} band (also of the A_2 class) was not surprising. We shall now consider the possibility that light could penetrate from other scattering geometries.

Some misorientation of the polarization of the exciting light may give rise to contributions of the components $\beta_{xz'z}$, $\beta_{xx'z}$, $\beta_{xyx'}$, and $\beta_{xyy'}$, and, in view of the finite angle of collection of the scattered light, there may be also contributions from $\beta_{z'yz}$, and $\beta_{y'yz}$, (the prime refers to the axis that appears because of misorientations; contributions of the components with two or three primed axes was ignored because of their smallness). Among possible components there are three nonzero ones ($\beta_{xx'z}$, $\beta_{xyx'}$, and $\beta_{y'yz}$) in the case of the A_2 vibrations and only one ($\beta_{xyy'}$) in the case of the A_1 vibrations.

The question arises whether the appearance of the A_1 vibration bands (201 and 464 cm^{-1}) in the $x(xyz)y$ geometry is due to the $\beta_{xyy'}$ component. This can be answered by comparing the intensities of the bands observed in the $x(xyz)y$ geometry and of the same bands in the $x(xyy)y$ geometry. It was found that in the latter geometry the 201 and 464 cm^{-1} bands were only 3–5 times stronger. Therefore, we could reliably conclude that the appearance of the 201 and 464 cm^{-1} bands belonging to the A_1 vibration could not be due to misorientation of the crystal and depolarization of light, but the main contribution to their intensity was due to the component $\bar{\beta}_{xyz}$ of the asymmetric part of the HRS tensor. It should be pointed out that the asymmetric part represented a considerable fraction compared with the components of the symmetric tensor. According to our estimates, the asymmetric part represented $\beta_{xyz} \approx (0.2$–$0.5)\beta_{xyy}$.

5.2. Asymmetry resulting from transposition of tensor indices

The components of a totally symmetric tensor are not affected by the transposition of the indices: $\beta^s_{mnl} = \beta^s_{mln} = \beta^s_{nml} = \beta^s_{nlm} = \beta^s_{lmn} = \beta^s_{lnm}$. However, if an allowance is made for the asymmetric part, these components cannot be equal. It follows from Sec. 5.1 that the contribution of the asymmetric part of the HRS intensity is low (it does not exceed a factor of 2) and its detection is difficult. In fact, as pointed out already, the intensities of HRS in α-quartz are generally low and a comparison of the tensor components obtained after transposition of indices should be made by comparing the intensities of the spectra recorded in different scattering geometries. Under these conditions it is possible to detect small changes in the intensities of the weak bands only by a comparison with an internal intensity standard. This standard was selected to be the hyper-Rayleigh scattering line at 355 nm, which was due to the summation of the frequencies of the exciting radiations ω_{i1} and ω_{i2} in the noncentrosymmetric crystal of α-quartz. The hyper-Rayleigh scattering line appeared in the HRS spectra for all the scattering geometries (for example, at the frequency $\omega_k = 0$ cm^{-1} in Figs. 2 and 5). Since the frequencies ω_{i1}, ω_{i2}, and $\omega_{i1} + \omega_{i2}$ were located in the transparency range of α-quartz, the Kleinman conditions were satisfied well for the hyper-Rayleigh scattering line,[13] i.e., the hyper-Rayleigh scattering intensity should not be affected by transposition of the tensor-component indices (see also Ref. 3). The hyper-Rayleigh scattering line was particularly suitable as an internal standard because its use automatically allowed for fluctuations of the exciting radiation with time and also excluded difficulties encountered in superimposing exactly the constrictions of the exciting beams ω_{i1} and ω_{i2} in different scattering geometries. It should be pointed out that in the selected scattering geometry the intensity of the hyper-Rayleigh scattering line did not vary between various points in a crystal.

Using this internal standard we were able to detect reliably slight changes in the intensities of the HRS bands, as illustrated by the example of the intensity of the 128 cm^{-1} of the E vibration (Fig. 5). We selected those scattering geometries in which the spectra were distorted least by the anisotropy and optical activity of the crystal. In the first geometry both exciting beams were polarized along z [$x(xzz)y$ geometry], whereas in the other case the polarizations of the two beams were mutually orthogonal [$y(zzx)x$ geometry]. In the first case the HRS intensity was governed by the β_{xxz}

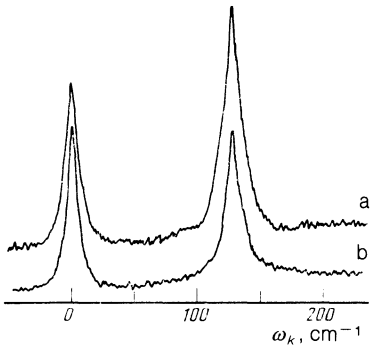

FIG. 5. Hyper-Raman spectra of α-quartz obtained in the $x(xzz)y$ (a) and $y(zzx)x$ (b) geometries.

component, whereas in the second it was governed by the β_{zzx} component. The spectrograms (Fig. 5) were normalized in respect of the intensity, so that the intensities of the hyper-Rayleigh scattering lines were the same in both spectra. In this case the intensities of the 128 cm^{-1} line were different. The relative change in the intensity of the 128 cm^{-1} line in the two geometries did not exceed a factor of 1.5.

6. CONCLUSIONS

Two-frequency excitation was used for the first time to study the HRS spectra of α-quartz and the effects of the intensity anisotropy and of the asymmetry of the HRS tensor.

Although the frequencies of the exciting and scattered light were far from the electronic absorption region of α-quartz ($\omega_{i1}/\omega_\alpha \approx 0.1, \omega_{i2}/\omega_\alpha \approx 0.2$, and $\omega_s/\omega_\alpha \approx 0.35$), we nevertheless detected the contribution of the asymmetric part of the HRS tensor representing a considerable fraction of the contribution of the totally symmetric part. We could expect the asymmetric contribution to rise on increase in the ratio $\omega_{s,i}/\omega_\alpha$. Therefore, in real experiments in which the ratio in question could be $\gtrsim 0.8$ (for example, in the case of rutile crystal when HRS is excited by the 1064 nm line), the relative contribution of the asymmetric part may be quite large. Therefore, in contrast to RS for which the asymmetric part can be significant only in the direct vicinity of an electronic absorption band ($\omega_\alpha - \omega_s \lesssim \omega_k$), in the case of HRS it is practically always necessary to allow for the possibility of a contribution from the asymmetric part $\bar{\beta}_{mnl}$ of the tensor.

[1]S. A. Akhmanov and D. N. Klyshko, Pis'ma Zh. Eksp. Teor. Fiz. **2**, 171 (1965) [JETP Lett. **2**, 108 (1965)].
[2]S. S. Jha and J. W. F. Woo, Nuovo Cimento B **2**, 167 (1971).
[3]D. A. Long and L. Stanton, Proc. R. Soc. (London) Ser. A **318**, 441 (1970).
[4]J. H. Christie and D. J. Lockwood, J. Chem. Phys. **54**, 1141 (1971).
[5]G. Placzek, The Rayleigh and Raman Scattering, US AEC Report UCRL-Trans-526(L), 1962, § 14.
[6]J. F. Scott and S. P. S. Porto, Phys. Rev. **161**, 903 (1967).
[7]F. Gervais and B. Piriou, Phys. Rev. B **11**, 3944 (1975).
[8]B. Dorner, H. Grimm, and H. Rzany, J. Phys. C **13**, 6607 (1980).
[9]S. J. Cyvin, J. E. Rauch, and J. C. Decius, J. Chem. Phys. **43**, 4083 (1965).
[10]V. N. Denisov, B. N. Mavrin, V. B. Podobedov, and Kh. E. Sterin, Zh. Eksp. Teor. Fiz. **75**, 684 (1978); **84**, 1266 (1983) [Sov. Phys. JETP **48**, 344 (1978); **57**, 733 (1983)].
[11]S. M. Kostritskiĭ, A. E. Semenov, and E. V. Cherkasov, Fiz. Tverd. Tela (Leningrad) **23**, 2090 (1981) [Sov. Phys. Solid State **23**, 1219 (1981)].
[12]J. F. Nye, *Physical Properties of Crystals*, Clarendon Press, Oxford, 1957 (Russ. transl., Mir, M., 1967), Chap. XIV.
[13]N. Bloembergen, *Nonlinear Optics*, Benjamin, New York, 1965 (Russ. transl., Mir, M., 1966), Chap. 1, § 3.

Translated by A. Tybulewicz